

The High Energy cosmic-Radiation Detector (HERD) Trigger System

M. A. Velasco,^{a,*} T. Bao,^b E. Berti,^c V. Bonvicini,^d J. Casaus,^a F. Giovacchini,^a X. Liu,^b R. Marco,^a J. Marín,^a G. Martínez,^a N. Mori,^c A. Oliva,^e L. Pacini,^c Z. Quan,^b Z. Tang,^b M. Xu,^b G. Zampa^d and N. Zampa^d on behalf of the HERD Collaboration
(a complete list of authors can be found at the end of the proceedings)

^a*Centro de Investigaciones Energéticas, Medioambientales y Tecnológicas (CIEMAT),
Avda. Complutense 40, E-28040, Madrid, Spain*

^b*Key Laboratory of Particle Astrophysics, Institute of High Energy Physics, Chinese Academy of Sciences,
Beijing 100049, China*

^c*Istituto Nazionale di Fisica Nucleare (INFN) Sezione di Firenze,
Via G. Sansone 1, I-50019 Sesto Fiorentino, Florence, Italy*

^d*Istituto Nazionale di Fisica Nucleare (INFN) Sezione di Trieste,
Padriciano 99, I-34012 Trieste, Italy*

^e*Istituto Nazionale di Fisica Nucleare (INFN) Sezione di Bologna,
Viale Carlo Berti Pichat, 6/2, 40127 Bologna BO, Italy*

E-mail: MiguelAngel.Velasco@Ciemat.es

The High Energy cosmic-Radiation Detection (HERD) facility is a next generation spaceborne detector to be installed onboard the Chinese Space Station for about 10 years.

HERD will address major problems in fundamental physics and astrophysics, providing precise measurements of charged-cosmic rays up to PeV energies, performing indirect searches for dark matter in the electron spectrum up to few tens of TeV and monitoring the gamma-ray skymap for surveys and transient searches.

HERD is composed of a 3D imaging calorimeter (CALO) surrounded by a scintillating fiber tracker (FIT), a plastic scintillator detector (PSD) and a silicon charge detector (SCD). In addition, a transition radiation detector (TRD) is placed on a lateral side to provide accurate energy calibration. Based on this innovative design, the effective geometric factor of HERD will be one order of magnitude larger than that of current space-based detectors.

The HERD trigger strategy is designed to accomplish the scientific goals of the mission, and is based on trigger definitions that rely on the energy deposited in CALO and the PSD. The trigger performances are evaluated using a detailed Monte Carlo simulation that includes the latest HERD geometry.

In addition, alternative trigger definitions based on the event topology can be established thanks to the photodiode readout of CALO crystals. The feasibility of these topological triggers is also investigated and presented.

37th International Cosmic Ray Conference (ICRC 2021)

July 12th – 23rd, 2021

Online – Berlin, Germany

*Presenter

1. The HERD detector

The High Energy cosmic-Radiation Detector (HERD) is a future cosmic ray experiment planned to be installed onboard the Chinese Space Station (CSS) for a 10-year mission [1]. The instrument will follow a low Earth orbit with an inclination of 41.5° and an altitude between 340 and 450 km.

The primary scientific goals of the HERD experiment encompass the precise measurement of the spectra and composition of primary cosmic rays up to the *knee* region; the indirect search for signatures of dark matter annihilation through the precise measurement of the electron energy spectrum up to tens of TeV and its anisotropy; and gamma ray astronomy and transient monitoring. Therefore, HERD will address major problems in fundamental physics and astrophysics with the precise measurements of charged cosmic-rays and gamma-rays. To achieve these goals, the HERD experiment features a large acceptance detector based on an innovative concept.

HERD consists of several sub-detectors that provide accurate determination of the particle properties (figure 1). The detector comprises a 3D imaging calorimeter (CALO) made of cubic LYSO crystals which, in total, provide about 55 radiation lengths and 3 nuclear interaction lengths. The calorimeter is surrounded by a scintillating fiber tracker (FIT) that allows for charge measurement and trajectory reconstruction; a plastic scintillator detector (PSD) which provides charge reconstruction and gamma identification; and a silicon charge detector (SCD) to have a precise determination of the particle charge. In addition, a transition radiation detector (TRD), located on one lateral side, provides accurate energy calibration.

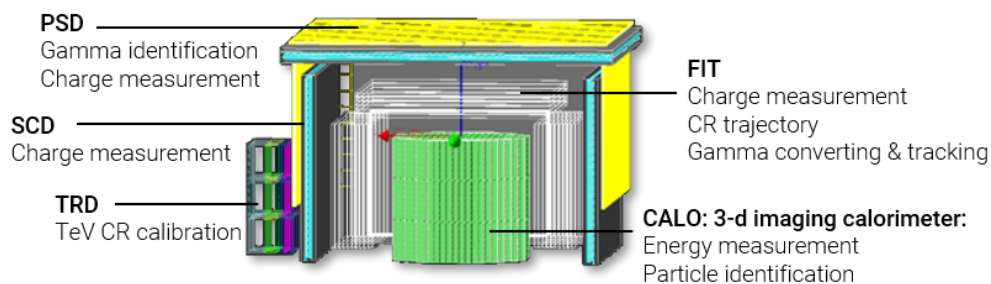


Figure 1: Transversal view of HERD sub-detectors layout.

HERD is designed to accept incident particles from both its top and four lateral faces thus providing an effective geometrical factor one order of magnitude larger than that of current experiments.

2. Baseline trigger strategy

The large geometrical acceptance of the system requires detailed studies to define an efficient trigger system, which is able to identify the event samples for science and calibration purposes and keep the trigger rate to the level required by the acquisition system.

The trigger strategy is defined to fulfill the scientific goals of the HERD experiment according to the particle species and energies of the required event samples.

The HERD trigger system is based on two kinds of configurations:

1. Science mode - Global Trigger, composed of the logical OR of individual sub-triggers:

- *High Energy trigger* (HE), which requires high energy deposition in CALO.
- *Low Energy Gamma trigger* (LEG), which requires low energy deposition in CALO and PSD veto to suppress mainly the proton background.
- *Low Energy Electron trigger* (LEE), which requires low energy deposition in CALO and provides calibration of the TRD response curve.
- *Unbiased trigger* (UNB), which requires low energy deposition in CALO and is based on a prescaled sample of events (1/1000) for trigger efficiency computation.

2. Calibration mode

- *Standalone calibration* (CALIB), which requires low energy deposition in CALO and aims to select penetrating charged particles to equalize the response of the CALO cells. It is operated in a geographical band of latitudes from -20° to $+20^\circ$ around the Earth's equator.

3. Study of trigger performances

The performances of the baseline trigger definitions have been evaluated in terms of the trigger acceptances and expected trigger rates using Monte Carlo simulated samples. These samples are produced by means of HerdSoftware [2], a dedicated framework based on Geant4 for Monte Carlo simulation, event reconstruction and data analysis for the HERD experiment.

The simulated samples for the trigger studies include different particle species (protons, electrons, helium, carbon and gammas) and logarithmically spaced energy points ranging from 0.1 GeV to 8 TeV. The Monte Carlo generation is performed using the latest geometry currently implemented in HerdSoftware.

A systematic procedure to evaluate the trigger acceptances and the expected trigger rates has been followed. For the computation of the trigger rates, the input particle fluxes are obtained from GALPROP [3] spectra tuned to the latest AMS-02 results. At low energies, the force field approximation [4] is used to account for the solar modulation, where two potentials are used to investigate the trigger rates in two extreme cases: $\phi_{\text{MIN}} = 300$ MV, for the solar minimum; and $\phi_{\text{MAX}} = 1200$ MV, for the solar maximum. In addition, the orbital parameters of the recently launched Tianhe core module of the CSS [5] are used for the trigger rate computation.

For downward-going protons, the results obtained for the trigger acceptances of the baseline definitions are presented in figure 2-left. In particular, due to its importance in the measurement of high energy cosmic rays, the HE trigger exhibits a fast rise above the energy threshold in CALO and an almost flat acceptance, about $3 \text{ m}^2\text{sr}$, for energies above 80 GeV. On the other hand, the expected proton HE trigger rate for the solar minimum is displayed in figure 2-right. As observed, the HE trigger rate exhibits a uniform behavior along the CSS orbit, with an average trigger rate of 49.5 Hz and a maximum of 50 Hz.

The results of the expected trigger rates for protons are presented in table 1.

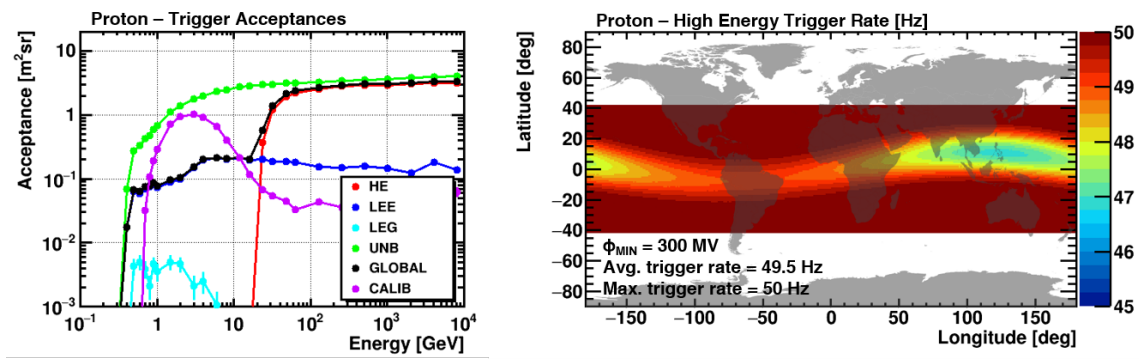


Figure 2: (Left) Trigger acceptances for downward-going protons. (Right) Proton High Energy trigger rate map for the solar minimum. The colored band corresponds to the geographical latitudes covered by the CSS orbit and the gradient of colors quantify the trigger rate at the different geographical positions.

Table 1: Expected trigger rates for downward-going protons.

Protons	Avg. Rate [Hz]	Max. Rate [Hz]
HE	49.5	50.0
LEE	72.5	311.2
LEG	0.5	8.1
UNB	0.9	3.6
GLOBAL	123.1	372.5
CALIB	26.4	94.3

4. Feasibility of a topological trigger

The possibility of instrumenting a subsample (1/N) of the LYSO crystals with an additional system of photodiodes and readout electronics provides an alternative to the standard readout of CALO based on fibers coupled to PMTs. This photodiode readout of the CALO LYSO crystals provides topological trigger capabilities that may complement the baseline trigger definitions based on the energy deposition in CALO.

The differences in the shower shape in CALO can be exploited to separate electrons and protons using the PD readout. A simple programmable logic (based on the total multiplicity or x,y,z-projection multiplicities) built from individual PD self-trigger signals provides enhanced particle identification as long as a low threshold ($\leq 1 \text{ MIP}$) can be set.

Therefore, the photodiode readout offers the possibility to design dedicated triggers for specific particle species and energy ranges based on the event topology in terms of the aforementioned multiplicities. Currently, four trigger definitions have been investigated:

- *High Energy Topological trigger* (HET), exploits the correspondence between the total energy deposited in CALO and the total multiplicity to provide an alternative high energy trigger based only on the event topology.
- *Low Energy Electron Topological trigger* (LEET), provides a high acceptance trigger for

electrons at low energies with strong proton suppression, which may constitute additional samples for science and calibration purposes.

- *High Energy Electron Topological trigger* (HEET), for electrons at intermediate energies, thus providing an overlap between the LEET and HET triggers.
- *MIP Topological trigger* (MIPT), exploits the correlation between the total number of fired crystals and the depth in LYSO, thus allowing for a selection of MIP events that provide energy calibration for different lengths in CALO.

The performances of these topological trigger definitions have been investigated using a similar procedure as described in the previous section. The trigger acceptances for electrons and protons are displayed in figure 3.

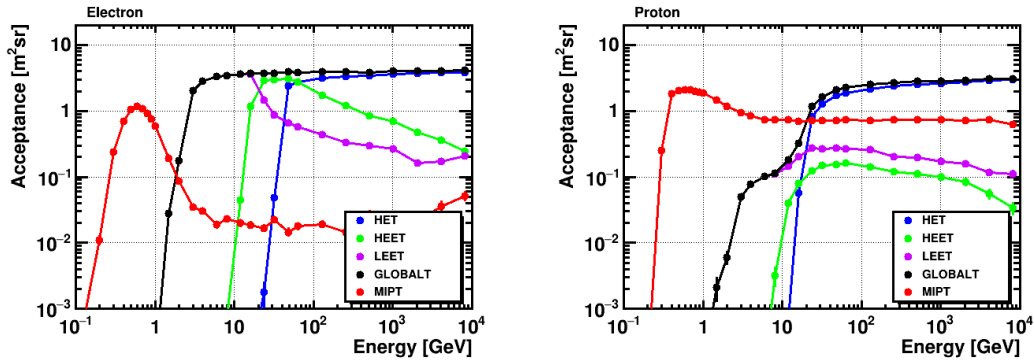


Figure 3: Acceptances of the topological trigger definitions for downward-going electrons (*left*) and protons (*right*).

5. Conclusions

The HERD experiment onboard the CSS constitutes the flagship of the next generation of cosmic ray detectors in space.

A novel design based on the possibility to accept particles from the top and lateral sides of HERD provides an effective geometrical factor one order of magnitude larger than that of current space-based detectors. This will allow to provide accurate measurements of charged cosmic rays and gamma-rays from few GeV to PeV energies and address major problems in fundamental physics and astrophysics.

The trigger strategy is designed to fulfill these scientific goals and provide meaningful samples for science and calibration purposes. The trigger logic is defined in terms of different sub-triggers based on the energy deposited in CALO and the PSD.

In addition, the photodiode readout of the CALO crystals provides an additional opportunity for alternative trigger definitions based on simple programmable logic in terms of the event multiplicities. Dedicated sub-triggers for specific particle species and energy ranges have been proposed and investigated.

References

- [1] Y. Dong, S. Zhang, G. Ambrosi (HERD Collaboration), *Overall Status of the High Energy Cosmic Radiation Detection Facility Onboard the Future China's Space Station*, [PoS ICRC2019 \(2020\) 062](#)
- [2] <http://herd.pg.infn.it/wiki/>
- [3] A. W. Strong, I. V. Moskalenko, V. S. Ptuskin. *Cosmic- Ray Propagation and Interactions in the Galaxy*. *Ann.Rev.Nucl.Part.Sci.*, 57(1):285-327 (2007) [[astro-ph.HE/0701517](#)]
- [4] L. J. Gleeson, W. I. Axford, *Solar Modulation of Galactic Cosmic Rays*, *Ap.J* 154:1011 (1968)
- [5] <https://www.n2yo.com/satellite/?s=48274>

Full Authors List: HERD Collaboration

O. Adriani²⁶, F. Alemanno²⁷, R. Aloisio²⁷, C. Altomare²³, G. Ambrosi³⁴, Q. An¹⁰, M. Antonelli⁴⁵, P. Azzarello³⁷, L. Bai⁸, Y.L. Bai³, T.W. Bao¹, M. Barbanera³⁴, F.C.T. Barbato²⁷, P. Bernardini³⁰, E. Berti²⁶, B. Bertucci³⁵, X.J. Bi¹, G. Bigongiari³⁶, M. Bongio²⁶, V. Bonvicini⁴⁵, P. Bordas⁴⁰, V. Bosch-Ramon⁴⁰, S. Bottai²⁵, P. Brogi³⁶, F. Cadoux³⁷, D. Campana³¹, W.W. Cao³, Z. Cao¹, J. Casaus³⁹, E. Catanzani³⁵, P. W. Cattaneo³³, J. Chang^{9,13}, Y.H. Chang²¹, G.M. Chen¹, Y. Chen¹⁵, F. Cianetti³⁵, A. Comerma^{40,41}, D. Cortis²⁸, X.H. Cui¹³, X.Z. Cui¹, C. Dai⁵, Z.G. Dai¹⁵, R. D'Alessandro²⁶, S. De Gaetano²⁴, I. De Mitri²⁷, F. de Palma³⁰, V. Di Felice⁵⁰, A. Di Giovanni²⁷, M. Di Santo²⁷, L. Di Venere²⁴, J.N. Dong^{6,7}, Y.W. Dong¹, G. Donvito²³, M. Duranti³⁴, D. D'Urso⁴⁹, C. Evoli²⁷, K. Fang¹, L. Fariña⁴², Y. Favre³⁷, C.Q. Feng¹⁰, H. Feng¹⁶, H.B. Feng⁵, Z.K. Feng⁵, N. Finetti²², V. Formato⁵⁰, J. M. Frieden⁴⁴, P. Fusco²⁴, J.R. Gao³, F. Gargano²³, D. Gascon-Fora⁴⁰, D. Gasparrini⁵⁰, N. Giglietto²⁴, F. Giovacchini³⁹, S. Gomez⁴⁰, K. Gong¹, Q.B. Gou¹, R. Guida⁴⁶, D.Y. Guo¹, J.H. Guo⁹, Y.Q. Guo¹, H.H. He¹, H.B. Hu¹, J.Y. Hu^{1,2}, P. Hu^{1,2}, Y.M. Hu⁹, G.S. Huang¹⁰, J. Huang¹, W.H. Huang^{6,7}, X.T. Huang^{6,7}, Y.B. Huang⁵, Y.F. Huang¹⁵, M. Ionica³⁴, L. Jouvin⁴², A. Kotenko³⁷, D. Kyratzis²⁷, D. La Marra³⁷, M.J. Li^{6,7}, Q.Y. Li^{6,7}, R. Li³, S.L. Li^{1,2}, T. Li^{6,7}, X. Li⁹, Z. Li¹⁷, Z.H. Li^{1,2}, E.W. Liang⁵, M.J. Liang^{1,2}, C.L. Liao⁸, F. Licciulli²³, S.J. Lin¹, D. Liu^{6,7}, H.B. Liu⁵, H. Liu⁸, J.B. Liu¹⁰, S.B. Liu¹⁰, X. Liu^{1,2}, X.W. Liu⁵, Y.Q. Liu¹, F. Loparco²⁴, S. Loporchio²³, X. Lu⁵, J.G. Lyu⁴, L.W. Lyu³, P. Maestro³⁶, E. Mancini³⁴, R. Manera⁴⁰, J. Marin³⁹, P. S. Marrocchesi³⁶, G. Marsella⁵³, G. Martinez³⁹, M. Martinez⁴², D. Marzullo⁴⁷, J. Mauricio⁴⁰, E. Mocchiutti⁴⁵, G. Morettini³⁵, N. Mori²⁵, L. Mussolin³⁵, M. Nicola Mazziotta²³, A. Oliva⁵¹, D. Orlandi²⁸, G. Osteria³¹, L. Pacini²⁵, B. Panico³¹, F.R. Pantalei²⁴, S. Papa⁴⁶, P. Papini²⁵, J.M. Paredes⁴⁰, A. Parenti²⁷, M. Pauluzzi³⁵, M. Pearce⁴³, W.X. Peng¹, F. Perfetto³¹, C. Perrina⁴⁴, G. Perrotta⁴⁶, R. Pillera²⁴, C. Pizzolotto⁴⁵, R. Qiao¹, J.J. Qin³, L. Quadran^{51,52}, Z. Quan¹, A. Rappoldi³³, G. Raselli³³, X.X. Ren^{6,7}, F. Renno⁴⁶, M. Ribo⁴⁰, J. Rico⁴², M. Rossella³³, F. Ryde⁴³, A. Sanmukh⁴⁰, V. Scotti³², D. Serini²³, D.L. Shi³, Q.Q. Shi^{6,7}, L. Silveri²⁷, O. Starodubtsev²⁵, D.T. Su¹², M. Su²⁰, D. Sukhonos³⁷, A. Suma⁴⁶, X.L. Sun¹, Z.T. Sun^{1,2}, A. Surdo²⁹, Z.C. Tang¹, A. Tiberio²⁶, A. Tykhonov³⁷, V. Vagelli⁴⁸, E. Vannuccini²⁵, M. Velasco³⁹, R. Walter³⁸, A.Q. Wang^{6,7}, B. Wang³, J.C. Wang¹⁴, J.M. Wang¹, J.J. Wang^{1,2}, L. Wang¹³, M. Wang^{6,7}, R.J. Wang¹, S. Wang⁹, X.Y. Wang¹⁵, X.L. Wang¹⁰, Z.G. Wang¹, D.M. Wei⁹, J.J. Wei⁹, B.B. Wu¹, J. Wu¹⁹, L.B. Wu²⁷, X. Wu³⁷, X.F. Wu⁹, Y.L. Xin⁸, M. Xu¹, Z.Z. Xu¹⁰, H.R. Yan¹⁷, Y. Yang³, P.F. Yin¹, Y.W. Yu¹⁸, Q. Yuan⁹, G. Zampa⁴⁵, N. Zampa⁴⁵, M. Zha¹, C. Zhang¹, F.Z. Zhang^{1,2}, L. Zhang¹, L. Zhang¹¹, L.F. Zhang^{1,2}, S.N. Zhang^{1,2}, Y. Zhang⁹, Y.L. Zhang¹⁰, Z.G. Zhao¹⁰, J.K. Zheng³, Y.L. Zhou⁵, F.R. Zhu⁸, and K.J. Zhu⁴

¹ Key Laboratory of Particle and Astrophysics, Chinese Academy of Sciences, Beijing, China

² University of Chinese Academy of Sciences, Beijing, China

³ Xi'an Institute of Optics and Precision Mechanics of CAS, Xi'an, China

⁴ Institute of High Energy Physics, Chinese Academy of Sciences, Beijing, China

⁵ School of Physical Science and Technology, Guangxi University, Nanning, China

⁶ Institute of Frontier and Interdisciplinary Science, Shandong University, Qingdao, China

⁷ Key Laboratory of Particle Physics and Particle Irradiation, Ministry of Education, China

⁸ School of Physical Science and Technology, Southwest Jiaotong University, Chengdu, China

⁹ Key Laboratory of Dark Matter and Space Astronomy, Purple Mountain Observatory, Chinese Academy of Sciences, Nanjing 210023, China

¹⁰ Department of Modern Physics, University of Science and Technology of China, Hefei, China

¹¹ Department of Astronomy, Yunan University, Kunming, China

¹² North Night Vision Technology co. Ltd., Kunming, China

¹³ National Astronomical Observatories, Chinese Academy of Sciences, Beijing 100101, China

¹⁴ Yunnan Astronomical Observatory, Chinese Academy of Sciences, Kunming, China

¹⁵ School of Astronomy and Space Science, Nanjing University, Nanjing, China

¹⁶ Department of Astronomy, Tsinghua University, Beijing, China

¹⁷ Department of Astronomy, Peking University, Beijing, China

¹⁸ Institute of Astrophysics, Central China Normal University, Wuhan, China

¹⁹ Department of Physics, China University of Geosciences, Wuhan, China

²⁰ The University of Hong Kong, Hong Kong, China

²¹ Institute of Physics, Academia Sinica, Taipei, Taiwan

²² Università dell'Aquila and Istituto Nazionale di Fisica Nucleare, Sezione di Firenze, Firenze, Italy

²³ Istituto Nazionale di Fisica Nucleare, Sezione di Bari, Bari, Italy

²⁴ Dipartimento di Fisica "M.Merlin" dell'Università e del Politecnico di Bari, and Istituto Nazionale di Fisica Nucleare, Sezione di Bari, Bari, Italy

²⁵ Istituto Nazionale di Fisica Nucleare, Sezione di Firenze, Firenze, Italy

²⁶ Università di Firenze and Istituto Nazionale di Fisica Nucleare, Sezione di Firenze, Firenze, Italy

²⁷ Gran Sasso Science Institute, L'Aquila, Italy and INFN Laboratori Nazionali del Gran Sasso, Assergi, L'Aquila, Italy

²⁸ INFN Laboratori Nazionali del Gran Sasso, L'Aquila, Italy

²⁹ Istituto Nazionale di Fisica Nucleare, Sezione di Lecce, Lecce, Italy

³⁰ Università del Salento and Istituto Nazionale di Fisica Nucleare, Sezione di Lecce, Lecce, Italy

³¹ Istituto Nazionale di Fisica Nucleare, Sezione di Napoli, Napoli, Italy

³² Università di Napoli "Federico II" and Istituto Nazionale di Fisica Nucleare, Sezione di Napoli, Napoli, Italy

- 33 Istituto Nazionale di Fisica Nucleare, Sezione di Pavia, Pavia, Italy
- 34 Istituto Nazionale di Fisica Nucleare, Sezione di Perugia, Perugia, Italy
- 35 Università degli Studi di Perugia and Istituto Nazionale di Fisica Nucleare, Sezione di Perugia, Perugia, Italy
- 36 Università di Siena and Istituto Nazionale di Fisica Nucleare, Sezione di Pisa, Pisa, Italy
- 37 Département de Physique Nucléaire et Corpusculaire (DPNC), Université de Genève, Genève, Switzerland
- 38 Department of Astronomy, University of Geneva, Geneva, Switzerland
- 39 Centro de Investigaciones Energéticas, Medioambientales y Tecnológicas (CIEMAT), E-28040 Madrid, Spain
- 40 Dept. Física Quàntica i Astrofísica, Institut de Ciències del Cosmos (ICCUB), Universitat de Barcelona (IEEC-UB), Barcelona, Spain
- 41 Universitat Pompeu Fabra (UPF), Barcelona, Spain
- 42 Institut de Física d'Altes Energies (IFAE), The Barcelona Institute of Science and Technology (BIST), E-08193 Bellaterra, Barcelona, Spain
- 43 KTH Royal Institute of Technology, Stockholm, Sweden
- 44 Institute of Physics, Ecole Polytechnique Fédérale de Lausanne (EPFL), Lausanne, Switzerland
- 45 Istituto Nazionale di Fisica Nucleare, Sezione di Trieste, Trieste, Italy
- 46 Università degli Studi di Napoli Federico II, Napoli, Italy
- 47 Università degli Studi di Trieste, Italy
- 48 Italian Space Agency and Istituto Nazionale di Fisica Nucleare, Sezione di Perugia, Perugia, Italy
- 49 Università degli Studi di Sassari and Istituto Nazionale di Fisica Nucleare, Sezione di Perugia, Perugia, Italy
- 50 Istituto Nazionale di Fisica Nucleare, Sezione di Roma Tor Vergata, Rome, Italy
- 51 INFN Sezione di Bologna, 40126 Bologna, Italy
- 52 INFN Sezione di Bologna, 40126 Bologna, Italy; Università di Bologna, 40126 Bologna, Italy
- 53 Dipartimento di Fisica e Chimica "E. Segrè" Università degli Studi di Palermo, Palermo, Italy and INFN sez. Catania, Catania, Italy